

## Effect of disorder on the magnetic properties of $\text{LaMn}_{0.5}\text{Fe}_{0.5}\text{O}_3$

Shekhar D. Bhamre, V. L. Joseph Joly, and P. A. Joy\*

*Physical and Materials Chemistry Division, National Chemical Laboratory, Dr. Homi Bhabha Road, Pune 411008, India*

(Received 30 March 2005; revised manuscript received 25 June 2005; published 18 August 2005)

Polycrystalline  $\text{LaMn}_{0.5}\text{Fe}_{0.5}\text{O}_3$  is synthesized by a low-temperature method and the magnetic properties of the resulting powder have been studied after annealing the sample in air at different temperatures in the range 200 °C–1350 °C. Room temperature Mössbauer spectroscopic studies show that the Fe ions are present in the +3 oxidation state in the material. However, the magnetic properties vary widely in an unexpected manner when samples are annealed at different temperatures. Zero field cooled magnetization studies show a cusp below 100 K, for the sample annealed at 200 °C, indicating a spin-glass-like or superparamagnetic behavior. However, this cusp disappears completely when the sample is annealed at 700 °C but still showing a magnetic hysteresis loop with reduced magnetization at low temperatures. The cusp again appears when the sample is annealed at higher temperatures with increasing low-temperature magnetization. EPR and IR spectroscopic studies indicate changes in the distribution of  $\text{Mn}^{3+}$  and  $\text{Fe}^{3+}$  ions in the lattice. The overall results can be explained in terms of random distribution of  $\text{Mn}^{3+}$  and  $\text{Fe}^{3+}$  ions in the lattice and formation of some magnetic clusters, with the degree of distribution of the ions varying for samples annealed at different temperatures.

DOI: [10.1103/PhysRevB.72.054426](https://doi.org/10.1103/PhysRevB.72.054426)

PACS number(s): 75.30.-m, 75.50.-y, 75.60.-d, 75.20.-g

### I. INTRODUCTION

Studies on divalent ion substituted rare earth manganites  $R_{1-x}D_x\text{MnO}_3$  ( $R$ =rare earth,  $D$ =alkaline earth), gained momentum in the recent past after they were found to show colossal magnetoresistance.<sup>1,2</sup> The transport and magnetic properties of the substituted manganites depend on their structure, composition, and the spin states of Mn. The substitution at the La site by divalent metal ions like Ca, Sr, etc., induces ferromagnetism in the antiferromagnetic insulator  $\text{LaMnO}_3$  because of the changes in the spin state of Mn from  $\text{Mn}^{3+}$  to  $\text{Mn}^{4+}$ . This shows that the substitution at the A site does ultimately affect the B site ion in the  $\text{ABO}_3$  perovskite structure. Therefore, the properties observed after La-site substitution can be partially reproduced by the direct substitution at the Mn site by proper ions. In fact such studies showed that ferromagnetism can be induced on direct substitution of Mn by Co, Ni, and Cr in  $\text{LaMnO}_3$ .<sup>3-6</sup> However, the latter case is much less explored due to the additional complexity arising from the possibility of more number of combinations of spin states of the ions in the Mn site.

The magnetic and transport properties of substituted perovskite manganites are mainly governed by the magic interplay of spin states exhibited by the manganese ion. Traditionally, the observed magnetic and transport properties have been explained using the double exchange (DE) model proposed by Zener on the basis of magnetic coupling between  $\text{Mn}^{3+}$  and  $\text{Mn}^{4+}$  ions, originating from the transfer of an electron between the two partially filled  $d$  shells with strong on-site Hund's rule coupling.<sup>7</sup> But later studies pointed out that DE alone cannot explain all the physics of these types of compounds. The other important factors governing the magnetic and transport behavior in manganites are the Jahn-Teller distortion and electron phonon coupling.<sup>8</sup>

The substitution of Mn by Fe in the  $\text{La}_{1-x}\text{D}_x\text{MnO}_3$  system, which is already ferromagnetic and metallic, destroys ferromagnetism and conductivity with increasing  $\text{Fe}^{3+}$  ion concentration.<sup>9-13</sup> The above observation, which is contra-

dicting the fact that  $\text{Fe}^{3+}-\text{O}-\text{Mn}^{3+}$  is expected to be one of the strongest ferromagnetic exchange interactions, is attributed to the random occupancy of high spin  $\text{Fe}^{3+}$  ion in the B site of the perovskite lattice. This increases the possibility of the antiferromagnetic  $\text{Fe}^{3+}-\text{O}-\text{Fe}^{3+}$  interactions. Studies on the effect of doping of different transition elements for Mn in  $\text{La}_{0.7}\text{Ca}_{0.3}\text{MnO}_3$  indicated some unusual effect on the substitution of  $\text{Fe}^{3+}$ .<sup>14</sup> From comparative studies on the role of impurity  $e_g$  levels on the properties of  $\text{Pr}_{0.5}\text{Ca}_{0.5}\text{MnO}_3$  doped with 5% of different elements, Hebert *et al.*<sup>15</sup> showed that doping elements with  $d^0$  and  $d^{10}$  configurations and dopants without  $d$  orbitals destroy ferromagnetic ordering and  $\text{Fe}^{3+}$  also belongs to this class in spite of its  $d^5$  electronic configuration. A similar effect has been observed in the case of direct Mn-site substitution also. Though ferromagnetism is induced on the substitution of the transition metal Co, Ni, and Cr for Mn in  $\text{LaMnO}_3$ , it was observed that the same effect is not produced on the substitution of Fe.<sup>16</sup>

Ueda *et al.* made artificial superlattices of  $\text{LaMnO}_3-\text{LaFeO}_3$  and found that the magnetic properties could be controlled by altering the ordering of Mn and Fe ions in the lattice.<sup>17</sup> Ferromagnetism, with a  $T_C$  of 230 K, is observed for stacking on the  $\langle 111 \rangle$  plane of  $\text{SrTiO}_3$  substrate whereas spin-glass-like behavior has been observed for  $\langle 100 \rangle$  and  $\langle 110 \rangle$  stacking. Further report by the same research group on the observation of ferromagnetism above room temperature in a thin film sample of  $\text{LaMn}_{0.5}\text{Fe}_{0.5}\text{O}_3$ , where the  $\text{Mn}^{3+}$  and  $\text{Fe}^{3+}$  ions were made to order, confirms the role of randomness in the occupancy of  $\text{Fe}^{3+}$  in determining the magnetic properties.<sup>18</sup> The driving force for the ordering of the ions in the B site of the perovskite lattice, when there are more than one type of ions present, is either the difference in the charge or the size (or both) of these ions. So, it is clear that, in a polycrystalline sample of  $\text{LaMn}_{0.5}\text{Fe}_{0.5}\text{O}_3$ , if Fe is present as trivalent high spin ion the compound is less likely to have ferromagnetic behavior due to the randomness in the occupancy, as trivalent Mn and Fe ions have identical ionic size (0.65 Å) (Ref. 19) and ionic charge. Though ferromag-

netism was not observed in polycrystalline  $\text{LaMn}_{0.5}\text{Fe}_{0.5}\text{O}_3$  in the earlier studies,<sup>16</sup> cluster-glass-like features with large difference between the field cooled and zero field cooled magnetization below 260 K are reported for this compound very recently.<sup>20</sup> The difference between the compounds in the above two reports is in the difference of the synthesis and processing conditions.

Our recent studies on polycrystalline  $\text{LaMn}_{0.5}\text{Co}_{0.5}\text{O}_3$  and  $\text{LaMn}_{0.5}\text{Ni}_{0.5}\text{O}_3$ ,<sup>21,22</sup> synthesized by a low-temperature method and annealed at different temperatures, showed the interplay of different spin states of Mn and the substituted ions in the two compounds and the effect of these parameters on their magnetic properties. These studies also showed how the processing conditions affect the magnetic properties, due to the changes in the spin states of Mn and the substituted ion. In the present study, polycrystalline  $\text{LaMn}_{0.5}\text{Fe}_{0.5}\text{O}_3$  is synthesized by a low temperature method and the magnetic properties of the resulting material have been evaluated after annealing at different temperatures in air. Mössbauer, EPR and IR spectroscopic studies were made to get more information on the changes in the magnetic properties and the state of Mn and Fe ions in the compound.

## II. EXPERIMENT

Polycrystalline  $\text{LaMn}_{0.5}\text{Fe}_{0.5}\text{O}_3$  was prepared by a low temperature method, as reported previously.<sup>23</sup> The powder sample obtained by the combustion method was divided into different parts and heated in air at 200 °C, 700 °C, and 1000 °C for 12 hours each, and at 1300 °C for 24 hours. The samples were furnace cooled to room temperature after heating at the respective temperatures. Part of the sample heated at 1300 °C was further heated at 1350 °C for 24 hours. These samples are labeled as LMF200, LMF700, LMF1000, LMF1300, and LMF1350. The samples were characterized by powder x-ray diffraction (XRD) studies using a Philips PW-1830 diffractometer. Magnetic measurements were made on a EG&G PAR 4500 vibrating sample magnetometer. Zero field cooled magnetization, in the temperature range 10–300 K and using a low magnetic field of 50 Oe, was measured while warming after cooling the samples from 300 to 10 K in zero applied field. The field dependence of magnetization was measured at 12 K up to a maximum field of 15 kOe. The EPR spectra were recorded at room temperature using a Bruker ER-200D-SRC EPR spectrometer. Room temperature  $\text{Fe}^{57}$  Mössbauer spectra were recorded on an Austin AS-600 Mössbauer spectrometer. IR spectra were recorded on a Perkin Elmer Spectrum-One FTIR spectrometer.

## III. RESULTS AND DISCUSSION

The powder XRD patterns of the  $\text{LaMn}_{0.5}\text{Fe}_{0.5}\text{O}_3$  samples annealed at 200 °C, 700 °C, and 1300 °C are shown in Fig. 1. The observed reflections in the XRD patterns correspond to that of a perovskite phase.<sup>24</sup> No extra reflections other than those of the single perovskite phase are observed, within the experimental limit, confirming the formation of single phase composition. All the three XRD patterns are

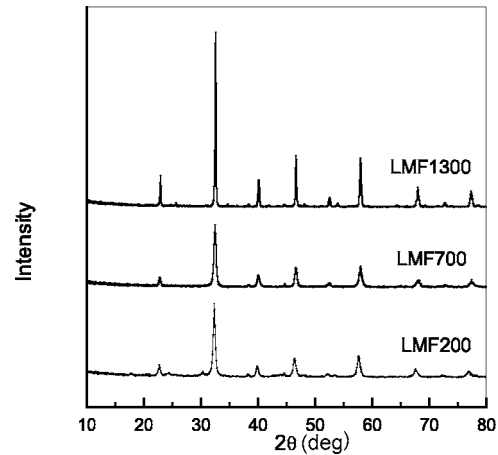


FIG. 1. Powder XRD patterns of  $\text{LaMn}_{0.5}\text{Fe}_{0.5}\text{O}_3$ , annealed at different temperatures.

identical, except for the broad reflections of the samples heated at lower temperatures, indicating the smaller crystallite sizes in these samples. The XRD patterns could be indexed to an orthorhombic perovskite structure and the lattice parameters were found to be comparable to the values reported.<sup>25</sup> Since both the end phases  $\text{LaMnO}_3$  and  $\text{LaFeO}_3$  have orthorhombic perovskite structures,  $\text{LaMn}_{0.5}\text{Fe}_{0.5}\text{O}_3$  is also expected to be orthorhombic.

Figure 2 shows the zero field cooled (ZFC) magnetization curves of the  $\text{LaMn}_{0.5}\text{Fe}_{0.5}\text{O}_3$  samples annealed at different temperatures, measured in a magnetic field of 50 Oe. A broad cusp at 68 K is observed for the sample annealed at 200 °C (LMF200). This feature is completely disappeared after annealing the sample at 700 °C (LMF700), as shown in the inset of Fig. 2. When the sample is heated at 1000 °C (LMF1000), a broad cusp appears at  $\sim 23$  K with a shoulder in the temperature region where a cusp is observed for LMF200. Further heating the sample at still higher temperatures enhances the feature at 68 K and at lower temperatures. Another interesting feature is the increasing magnetization at higher temperatures. For the sample heated to 1300 °C (LMF1300), the magnetization starts increasing below 200 K and this temperature is enhanced to 250 K, with enhanced

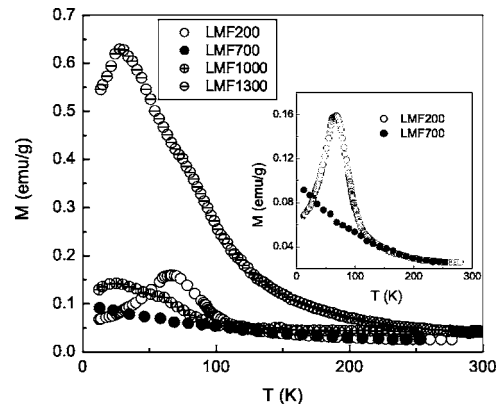


FIG. 2. ZFC magnetization curves of  $\text{LaMn}_{0.5}\text{Fe}_{0.5}\text{O}_3$ , for samples annealed at different temperatures. Inset, comparison of the ZFC magnetization behavior of LMF200 and LMF700.

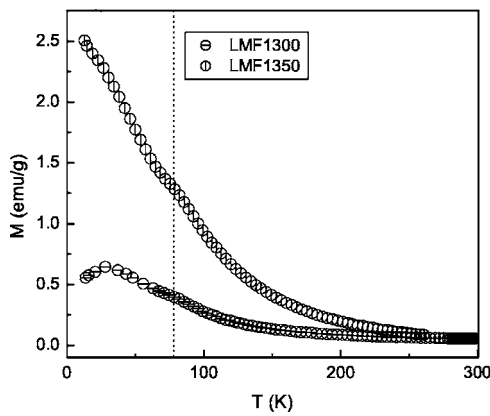


FIG. 3. Comparison of the ZFC magnetization curves of  $\text{LaMn}_{0.5}\text{Fe}_{0.5}\text{O}_3$ , for samples annealed at 1300 and 1350 °C. The vertical dotted line corresponds to the temperature at which a cusp is observed for LMF200.

magnetization at low temperatures as shown in Fig. 3, for the sample annealed at 1350 °C (LMF1350). The magnetization curve of LMF1300 is similar to that reported by De *et al.*<sup>20</sup>

Magnetization measurement as a function of magnetic field was performed at 12 K for the different samples. Figure 4 shows the initial magnetization curves of the samples annealed at different temperatures. There are some interesting aspects observed for all samples. LMF200 shows a magnetization curve similar to that of a superparamagnetic system, where the magnetization continuously increases at higher fields. Though LMF700 did not show any features in its ZFC magnetization data, still a superparamagnetic behavior is observed for this sample, with reduced magnetization when compared to that of LMF200. Annealing the sample above 700 °C enhances the low temperature magnetization. A sharper increase in the magnetization is observed for LMF1000 and LMF1300 at low magnetic fields, with larger magnitude of magnetization for LMF1300. Though a large increase in the ZFC magnetization is observed at low tem-

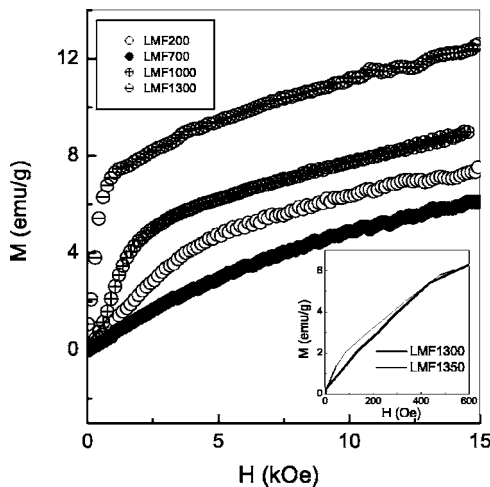


FIG. 4. Initial magnetization curves of  $\text{LaMn}_{0.5}\text{Fe}_{0.5}\text{O}_3$  at 12 K, for samples annealed at different temperatures. Inset, comparison of the initial magnetization curves of LMF1300 and LMF1350 at low magnetic fields.

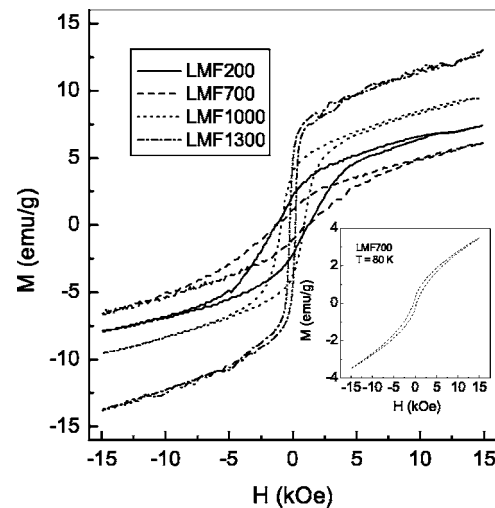


FIG. 5. Magnetic hysteresis loops of  $\text{LaMn}_{0.5}\text{Fe}_{0.5}\text{O}_3$  at 12 K, for samples annealed at different temperatures. Inset, MH behavior of LMF700 at 80 K.

peratures for LMF1350 when compared to LMF1300 (see Fig. 3), the initial magnetization curves of these two samples were found to be overlapping. For all samples, the magnetization increases linearly at higher magnetic fields. Another interesting observation is that the curves are almost parallel at higher magnetic fields for LMF1000 and LMF1300. With respect to the ZFC magnetization curves of these two samples, showing a shoulder at  $\sim 70$  K, it may be argued that these samples contain two magnetic phases, one with superparamagnetic behavior with a cusp at  $\sim 70$  K similar to that of LMF200 and another ferromagnetic phase.

The large difference in the low-temperature magnetization of LMF1300 and LMF1350, when measured in a field of 50 Oe, as shown in Fig. 3, can be explained on the basis of the initial magnetization at low magnetic fields. Previous studies have shown that there is a direct correlation between the initial magnetization at a given field measured at different temperatures and the temperature variation of the ZFC magnetization.<sup>26</sup> The initial magnetization curves of the two samples (measured at 12 K) at low magnetic fields are compared in the inset of Fig. 4. Though the magnitude of the magnetization is comparable at high magnetic fields ( $>500$  Oe), the magnetization at low magnetic fields is larger for LMF1350 and this will be reflected in the ZFC magnetization measurements made at low magnetic fields.

The magnetic hysteresis curves of the different samples are shown in Fig. 5. Interestingly, LMF700 shows some unexpected behavior. Although no feature is observed in the ZFC magnetization curve of this sample down to 12 K, a well-defined magnetic hysteresis curve, with a coercivity of 1170 Oe, is obtained for this sample. A magnetic hysteresis curve is observed for this sample even at a higher temperature of 80 K, with a coercivity of 390 Oe, as shown in the inset of Fig. 5. These well-defined magnetic hysteresis curves indicate that even though this sample is not showing any ferromagnetic transition, it is not truly paramagnetic, implying very small contribution from a ferromagnetic phase. The results favor a mixed phase problem in all

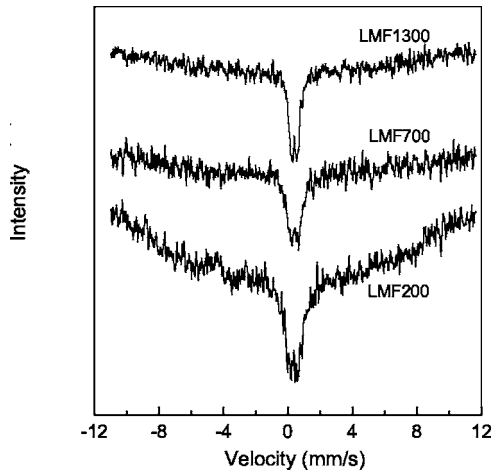


FIG. 6. Mössbauer spectra of  $\text{LaMn}_{0.5}\text{Fe}_{0.5}\text{O}_3$  at 300 K, for samples annealed at different temperatures.

samples, a ferromagnetic phase and a superparamagnetic phase whose contributions vary depending on the processing conditions.

Mössbauer spectra of the samples were recorded to identify the oxidation state of Fe in the different samples. The room temperature Mössbauer spectra of LMF200, LMF700, and LMF1300 are shown in Fig. 6. In all cases, only a doublet is observed in the spectra, indicating the paramagnetic nature of the samples at room temperature. The isomer shifts for LMF200, LMF700, and LMF1300 are obtained as 0.33, 0.43, and 0.40 mm/s, respectively. These values are those expected for  $\text{Fe}^{3+}$  ions and comparable to the values reported for the perovskite oxides  $\text{LaFeO}_3$ ,<sup>27</sup> and  $\text{SrFeO}_{2.5}$ ,<sup>28</sup> containing high spin  $\text{Fe}^{3+}$  ions, indicating that the Fe ions are present in their trivalent high-spin state in all the LMF samples. The isomer shift values are also comparable to the literature reported value for  $\text{LaMn}_{0.5}\text{Fe}_{0.5}\text{O}_3$ .<sup>20</sup> The spectra are identical to that reported by De *et al.*,<sup>20</sup> where  $\text{LaMn}_{0.5}\text{Fe}_{0.5}\text{O}_3$  synthesized at a low temperature and heated to 950 °C exhibits a large difference between the FC and ZFC magnetizations below 260 K. The latter observation is explained in terms of some local magnetic ordering. Tong *et al.*<sup>24</sup> have suggested the possibility of double exchange between  $\text{Mn}^{3+}$  ( $d^4$ ) and  $\text{Fe}^{3+}$  ( $d^5$ ) to explain the origin of ferromagnetism in  $\text{LaMn}_{1-x}\text{Fe}_x\text{O}_3$  ( $x \leq 0.4$ ) where similar doublet and isomer shift are observed. What is more interesting is the fact that the isomer shift initially increases to a larger value and then decreases. This is possible if the local environment of the  $\text{Fe}^{3+}$  ions is changed which affects the  $s$ -electron density. It may be assumed that the changes are due to the variation in the degree of distribution of the  $\text{Fe}^{3+}$  ions in the lattice, so that larger shift is observed when the disorder is more, as reported for other systems.<sup>29,30</sup>

The EPR spectra of the three samples LMF200, LMF700 and LMF1300 are shown in Fig. 7. There are large changes in the intensities and widths of the spectra when the samples are heated at higher temperatures. On the other hand, the resonance field remains the same for all three samples. For LMF700, the intensity of the EPR signal is reduced to almost half of that of LMF200 whereas the peak-to-peak linewidth

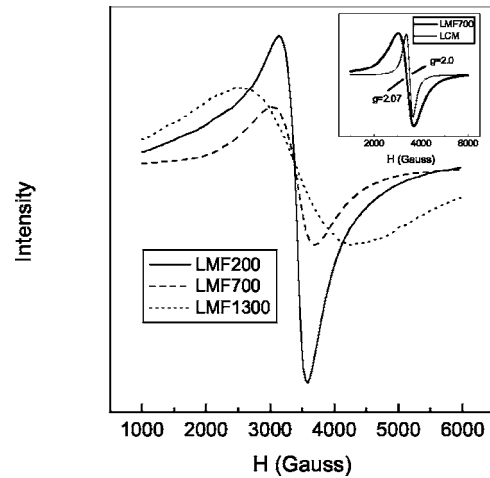


FIG. 7. EPR spectra of  $\text{LaMn}_{0.5}\text{Fe}_{0.5}\text{O}_3$  at 300 K, for samples annealed at different temperatures. Inset, comparison of the EPR spectra of LMF700 and  $\text{La}_{0.7}\text{Ca}_{0.3}\text{MnO}_3$  (LCM).

is increased from 448 to 655 Gauss. For LMF1300, the EPR signal becomes extremely broad with a peak-to-peak linewidth of 1790 Gauss. Although the signal becomes broad, the intensity is increased when compared to that of LMF700. In the La-site substituted manganites, where the EPR signal is due to the  $\text{Mn}^{3+}/\text{Mn}^{4+}$  pairs or interaction, the  $g$  value is close to 2.0. EPR signal from  $\text{Fe}^{3+}$  centers is also expected to give a  $g$  value of  $\sim 2.0$ . However, the  $g$  values are close to 2.07 for all three samples and this indicates that  $\text{Mn}^{3+}/\text{Fe}^{3+}$  pairs are responsible for resonance.

The relative integrated area under the curve is decreased from 2.4 (LMF200) to 1 (LMF700) and then increased to 3.9 (LMF1300). The area under the resonance curve is related to the number of unpaired spins contributing to paramagnetic susceptibility. Mössbauer spectral data clearly indicate that the Fe ions are present in their high-spin trivalent oxidation states. In fact the changes in the intensities and area under the curves of the EPR signals are directly correlated with the changes in the magnitude of the magnetization at low temperatures. Thus the initial decrease and further large increase in the susceptibility may be explained in terms of the corresponding changes in the  $\text{Mn}^{3+}/\text{Fe}^{3+}$  interactions. Assuming that only  $\text{Mn}^{3+}$  and  $\text{Fe}^{3+}$  ions are present in all the samples, the changes in the EPR data may be explained in terms of the distribution of these ions in the perovskite lattice. This degree of distribution is then responsible for the magnetic properties also.

The changes in the peak-to-peak linewidth is a direct measure of the magnetic exchange interactions and the linewidth increases because of the weakening of the exchange field. For example, Gutierrez *et al.*<sup>11</sup> have reported that the width of resonance line increases with Fe content in  $\text{La}_{0.7}\text{Pb}_{0.3}\text{Mn}_{1-x}\text{Fe}_x\text{O}_3$ , and this corresponds to a decrease of the exchange narrowing, indicating lowering of the strength of the ferromagnetic interactions. Compositions with larger Fe content show spin-glass-like behavior due to the antiferromagnetic coupling between Mn and Fe ions forming

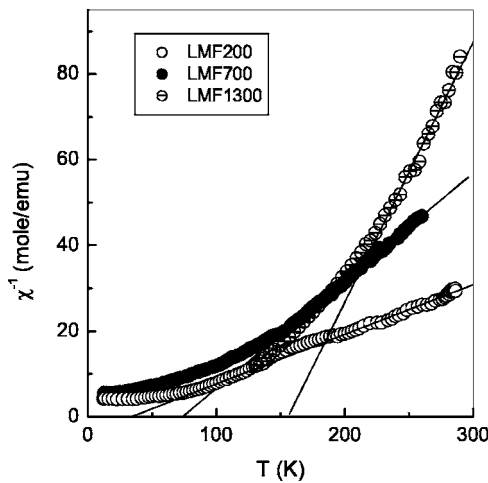


FIG. 8. Temperature variation of the inverse of the magnetic susceptibility of LMF200, LMF700, and LMF1300.

ferromagnetic clusters. On the other hand, Rubinstein *et al.*<sup>12</sup> have shown that in the case of  $\text{La}_{0.67}\text{Ca}_{0.33}\text{Mn}_{1-x}\text{M}_x\text{O}_3$  ( $M = \text{Co}, \text{Ni}$ ) the EPR linewidth increases drastically with Co substitution and weakens the signal whereas for Ni substitution the changes are very little. Rapid spin-lattice relaxation of Co ion and smaller spin-lattice relaxation mechanism for Ni are shown to be responsible for this difference. Blanco *et al.* observed that the effect of line broadening due to Fe substitution is in between that due to Co and Ni substitution for Mn in  $\text{Nd}_{0.7}\text{A}_{0.3}\text{Mn}_{1-x}\text{M}_x\text{O}_3$  ( $A = \text{Pb}, \text{Cd}; M = \text{Co}, \text{Ni}$ ).<sup>13</sup>

Although no strong magnetic signal is observed from low-field ZFC magnetization studies whereas field dependent magnetization at 12 K and 82 K show magnetic hysteresis loops indicating the contribution from some ferromagnetic phase, magnetic susceptibility studies show evidence for ferromagnetic exchange interactions in LMF700. Figure 8 shows the temperature dependence of the inverse of the magnetic susceptibility of LMF200 and LMF700, and LMF1300, measured in a magnetic field of 5000 Oe. Curie-Weiss behavior,  $\chi = C/(T - \Theta)$ , is observed for all samples at higher temperatures ( $> 150$  K). From least squares fit to the data in the linear region above 150 K, the effective paramagnetic moment,  $\mu_{\text{eff}} = 2.828\sqrt{C}$ , where  $C$  is the Curie constant, is obtained as 8.31, 5.64, 4.13, and 3.63  $\mu_B$ , respectively, for LMF200, LMF700, LMF1000, and LMF1300. LMF1350 gave almost identical value as that for LMF1300. Assuming that the samples contain only  $\text{Mn}^{3+}$  ( $S=2$ ) and  $\text{Fe}^{3+}$  ( $S=5/2$ ), as evidenced from Mössbauer and EPR studies, the spin only magnetic moment  $\mu_{\text{so}}$  for  $\text{LaMn}_{0.5}\text{Fe}_{0.5}\text{O}_3$  is calculated as  $\mu_{\text{so}} = [0.5\mu_{\text{Mn}}^2 + 0.5\mu_{\text{Fe}}^2]^{1/2} = 5.43\mu_B$ , where  $\mu = [4S(S+1)]^{1/2}$ . For a  $\text{Mn}^{4+}$  ( $S=3/2$ ) and  $\text{Fe}^{2+}$  ( $S=2$ ) combination,  $\mu_{\text{so}} = 4.42\mu_B$ . The experimental value of the magnetic moment of LMF700 is comparable to the spin-only value for the  $\text{Mn}^{3+}/\text{Fe}^{3+}$  combination indicating that Mn and Fe ions are present in their trivalent high-spin states. On the other hand, the large value of the experimental moment of LMF200 is similar to that observed for superparamagnetic systems and is indicative of ferromagnetic clusters in the sample. The ferromagnetic clusters are likely to contain  $\text{Mn}^{3+}$  and  $\text{Fe}^{3+}$  ions with  $\text{Mn}^{3+}\text{-O-Fe}^{3+}$  and/or  $\text{Mn}^{3+}\text{-O-Mn}^{3+}$  ferromag-

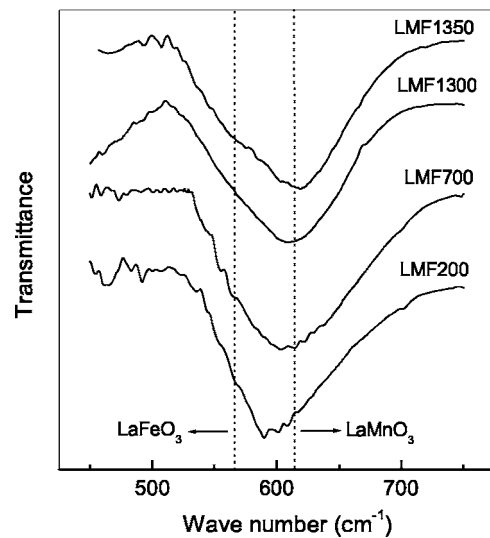


FIG. 9. IR spectra of  $\text{LaMn}_{0.5}\text{Fe}_{0.5}\text{O}_3$  samples annealed at different temperatures. The vertical dotted lines correspond to the vibrational frequencies of  $\text{LaMnO}_3$  and  $\text{LaFeO}_3$ , as indicated (from Ref. 25).

netic superexchange interactions. The paramagnetic Curie temperature,  $\Theta$ , is obtained as 34, 78, 117, and 156 K for LMF200, LMF700, LMF1000, and LMF1300, respectively. The positive values of  $\Theta$  are indicating the presence of ferromagnetic exchange interactions. The increasing value of  $\Theta$  with increasing annealing temperature is indicative of increasing strength of the ferromagnetic exchange interactions. The very low value of  $\Theta$  for LMF200 suggests that there are more antiferromagnetic interactions present in the samples, pointing to the formation of larger  $\text{Fe}^{3+}\text{-O-Fe}^{3+}$  clusters with antiferromagnetic exchange interactions. From the larger effective magnetic moment and smaller  $\Theta$  of this sample it can be assumed that the sample contains small Mn-rich clusters contributing to the superparamagnetic behavior. Then the larger values of  $\Theta$  and smaller values of the effective moments of LMF1000 and LMF1300 favor a conclusion in terms of larger Mn-rich clusters with stronger ferromagnetic exchange interactions. Thus from the magnetic susceptibility studies it can be concluded that the samples annealed at lower temperatures contain small Mn-rich clusters and larger Fe-rich clusters whereas the high-temperature annealed samples contain larger Mn-rich clusters.

Further evidence for the different degree of distribution of the  $\text{Mn}^{3+}$  and  $\text{Fe}^{3+}$  ions is obtained from IR spectroscopic studies. The IR spectra of the samples annealed at different temperatures are shown in Fig. 9. For the perovskite  $\text{ABO}_3$ , the B-O bond stretching vibration of the  $\text{BO}_6$  octahedra ( $\nu_1$  of the IR active  $F_{1u}$  mode of vibration) is observed in the 500–700  $\text{cm}^{-1}$  region.<sup>25,31</sup> Wu *et al.* have reported the IR spectral data of  $\text{LaMn}_{1-x}\text{Fe}_x\text{O}_3$  in the entire compositional range.<sup>25</sup> It has been shown that the band due to  $\nu_1$  stretching vibration observed at 610  $\text{cm}^{-1}$  for  $\text{LaMnO}_3$  is shifted to 568  $\text{cm}^{-1}$  for  $\text{LaFeO}_3$ , indicating that the Fe-O bond is more ionic. For  $\text{LaMn}_{0.5}\text{Fe}_{0.5}\text{O}_3$ , this band is observed at

606  $\text{cm}^{-1}$ . The decreasing vibrational frequency of the  $\nu_1$  mode has been shown to be resulting from the joint action of the Mn-O and Fe-O stretching vibrations, indicating that geometrical factors are more predominant than electronic factors in the system. Therefore, a symmetric band is expected if the  $\text{Mn}^{3+}$  and  $\text{Fe}^{3+}$  ions are distributed uniformly in the  $B$  site of the perovskite lattice and the band becomes nonsymmetric if the distribution is nonuniform or when clustering occurs. The spectra shown in Fig. 9 reveal changes in the structure of the vibrational band with annealing. For LMF200, the stretching frequency is  $\sim 600 \text{ cm}^{-1}$ , with a broad shoulder towards higher frequencies. However, a more symmetric band is observed for LMF700 at  $\sim 606 \text{ cm}^{-1}$ , similar to that reported by Wu *et al.*<sup>25</sup> For the samples annealed at higher temperatures (LMF1300 and LMF1350), the band is shifted to  $\sim 610 \text{ cm}^{-1}$ , with a shoulder at  $\sim 570 \text{ cm}^{-1}$ , which is clearly evident for LMF1350. Thus, LMF200 shows more features of  $\text{LaFeO}_3$  with minor features of  $\text{LaMnO}_3$  whereas LMF1350 shows major features of  $\text{LaMnO}_3$  and minor features due to  $\text{LaFeO}_3$ . LMF700 does not show any individual features of the end members. The IR spectral observations can be explained in terms of formation of clusters due to nonuniform distribution of  $\text{Mn}^{3+}$  and  $\text{Fe}^{3+}$  ions in the lattice. In LMF200, there are larger clusters involving  $\text{Fe}^{3+}$  and smaller clusters involving  $\text{Mn}^{3+}$  ions whereas in LMF1350, there are larger clusters involving  $\text{Mn}^{3+}$  and smaller clusters of  $\text{Fe}^{3+}$ . On the other hand, these ions are distributed more uniformly in LMF700, but probably with smaller clusters. The IR spectral data support the conclusions drawn from the magnetic susceptibility studies.

In the case of  $\text{LaMn}_{0.5}\text{Co}_{0.5}\text{O}_3$  and  $\text{LaMn}_{0.5}\text{Ni}_{0.5}\text{O}_3$  which are ferromagnetic with transition temperatures of 230 and 280 K,<sup>21,22</sup> respectively, for their high- $T_C$  phases, the magnetic ions are high-spin  $\text{Mn}^{3+}$  and low-spin  $\text{Co}^{3+}/\text{Ni}^{3+}$ . When these compounds are synthesized by the low-temperature method and annealed at 200 °C, the magnetic transition temperature is  $\sim 150 \text{ K}$  and the magnetic ions are present as  $\text{Mn}^{4+}$  and  $\text{Co}^{2+}/\text{Ni}^{2+}$ . It may be argued that the same scenario is possible in  $\text{LaMn}_{0.5}\text{Fe}_{0.5}\text{O}_3$  also with the contributions from  $\text{Mn}^{3+}/\text{Fe}^{3+}$  and  $\text{Mn}^{4+}/\text{Fe}^{2+}$  combinations giving rise to the observed magnetic properties for the samples annealed at different temperatures. However, as no evidence for  $\text{Fe}^{2+}$  was obtained in any of the samples from Mössbauer studies, the latter case can be ruled out. Also, the ESR spectral results are not in favor of  $\text{Mn}^{4+}/\text{Fe}^{2+}$  combination. Moreover, if it is assumed that  $\text{Mn}^{4+}$  and  $\text{Fe}^{2+}$  ions are present in LMF700 and these ions are distributed more uniformly in the lattice as deduced from the IR data, the experimental value of the effective magnetic moment obtained from the magnetic susceptibility data is much larger than the spin-only moment for the combination of these ions. Tong *et al.*,<sup>24</sup> from the magnetic, EPR and Mössbauer studies on  $\text{LaMn}_{1-x}\text{Fe}_x\text{O}_3$  up to  $x=0.4$ , have argued that double exchange interaction between  $\text{Mn}^{3+}$  and  $\text{Fe}^{3+}$  ions is responsible for ferromagnetism and that the  $\text{Fe}^{3+}$  may be in the intermediate spin state ( $t_{2g}^4 e_g^1$ ). However, studies on substitution of Fe for Mn in the  $A$ -site substituted CMR manganites show that  $\text{Fe}^{3+}$  ions are in their high-spin state. If it is assumed that  $\text{Mn}^{3+}$  and  $\text{Fe}^{3+}$  in their high-spin states are present in LMF700, then, because of the identical ionic sizes

of these ions, they will be distributed randomly in the  $B$  site of the perovskite lattice, so that some magnetic clusters will be formed. If the sizes of these clusters are very small, they will behave like superparamagnetic clusters. This way one can explain the origin of the superparamagnetic contribution in the sample. In fact, from studies on gradual substitution of  $\text{Fe}^{3+}$  for  $\text{Co}^{3+}$  in  $\text{LaMn}_{0.5}\text{Co}_{0.5}\text{O}_3$  it has been shown that a random distribution of  $\text{Mn}^{3+}$  and  $\text{Fe}^{3+}$  ions in the lattice is responsible for the destruction of long range ferromagnetic order in  $\text{LaMn}_{0.5}\text{Fe}_{0.5}\text{O}_3$ .<sup>32</sup>

The magnetic properties observed for the different samples can now be explained based on the above observations. In LMF200, the magnetic exchange interactions in the small Mn-rich clusters are ferromagnetic and large Fe-rich clusters are antiferromagnetic, as shown by Tanaka *et al.*<sup>33</sup> The peak observed in the ZFC magnetization curve is likely to be due to an antiferromagnetic transition or a superparamagnetic blocking transition due to the small Mn-rich ferromagnetic clusters. The large value of the effective magnetic moment of this sample and the lower value of the Weiss temperature because of antiferromagnetic contributions is an evidence for these conclusions. In the case of LMF700 showing some peculiar properties such as relatively large isomer shift, lower magnetization and EPR intensity, symmetric IR band, and  $\mu_{\text{eff}}$  closer to the spin-only value for  $\text{Fe}^{3+}/\text{Mn}^{3+}$  combination, the  $\text{Mn}^{3+}$  and  $\text{Fe}^{3+}$  ions are distributed somewhat uniformly in the lattice. However, still there is some contribution from a ferromagnetic-like phase as evidenced by the magnetic hysteresis loops with very low magnetization and this is likely to be due to some isolated Mn-rich clusters. In LMF1300, there are more and bigger ferromagnetic Mn-rich clusters so that the IR spectra resemble that of  $\text{LaMnO}_3$  and some antiferromagnetic Fe-rich clusters which give rise to the antiferromagnetic transition, observed as a small shoulder at  $\sim 70 \text{ K}$ , the temperature at which a transition is observed in LMF200. Annealing at higher temperatures leads to a kind of phase separation with more Fe-rich and Mn-rich clusters.

#### IV. CONCLUSIONS

Previous studies on  $\text{LaMn}_{0.5}\text{Fe}_{0.5}\text{O}_3$  have reported widely differing magnetic properties for the compound. No ferromagnetism in the compound was observed down to liquid nitrogen temperature in an earlier report whereas recent studies show weak ferromagnetic contributions below 250 K. The samples in the reported studies are made by different method and processed at different temperatures. We have studied the magnetic properties of the compound synthesized by a low-temperature method and heated at different temperatures in the temperature range 200 °C–1350 °C. Mössbauer, EPR and IR spectroscopic studies along with the magnetic data give information on the changes in the distribution of the  $\text{Mn}^{3+}$  and  $\text{Fe}^{3+}$  ions in the compound when processed at different temperatures. When Mn-rich and/or Fe-rich clusters with different sizes are formed, the compound shows predominant ferromagnetic or antiferromagnetic character whereas more uniform distribution of these ions makes it nonmagnetic. Thus, from the present study, the interesting

magnetic properties observed for polycrystalline  $\text{LaMn}_{0.5}\text{Fe}_{0.5}\text{O}_3$  can be explained based on a two-phase model where the degree of distribution of Mn and Fe ions in the lattice varies when the compound is annealed at different temperatures.

## ACKNOWLEDGMENTS

One of the authors (S.D.B.) is grateful to CSIR, India, for financial support. Financial assistance from DST, India, is also gratefully acknowledged.

\*Electronic address: pa.joy@ncl.res.in; URL: <http://www.ncl-india.org>

- <sup>1</sup>*Colossal Magnetoresistance, Charge Ordering and Related Properties of Manganese Oxides*, edited by C. N. R. Rao and B. Raveau (World Scientific, Singapore, 1998).
- <sup>2</sup>*Colossal Magnetoresistive Oxides*, edited by Y. Tokura (Gordon and Breach Science, Singapore, 2000).
- <sup>3</sup>A. Wold, R. J. Arnett, and J. B. Goodenough, *J. Appl. Phys.* **29**, 387 (1958).
- <sup>4</sup>J. B. Goodenough, A. Wold, R. J. Arnett, and N. Menyuk, *Phys. Rev.* **124**, 373 (1961).
- <sup>5</sup>G. Blasse, *J. Phys. Chem. Solids* **26**, 1969 (1965).
- <sup>6</sup>G. H. Jonker, *J. Appl. Phys.* **37**, 1424 (1966).
- <sup>7</sup>C. Zener, *Phys. Rev.* **82**, 403 (1951).
- <sup>8</sup>A. J. Millis, *Nature (London)* **392**, 147 (1998).
- <sup>9</sup>K. H. Ahn, X. W. Wu, K. Liu, and C. L. Chien, *Phys. Rev. B* **54**, 15299 (1996).
- <sup>10</sup>L. Righi, P. Gorria, M. Insausti, J. Gutierrez, and J. M. Barandiaran, *J. Appl. Phys.* **81**, 5767 (1997).
- <sup>11</sup>J. Gutierrez, A. Pena, J. M. Barandiaran, J. L. Pizarro, T. Hernandez, L. Lezama, M. Insausti, and T. Rojo, *Phys. Rev. B* **61**, 9028 (2000).
- <sup>12</sup>M. Rubinstein, D. J. Gillespie, J. E. Snyder, and T. M. Tritt, *Phys. Rev. B* **56**, 5412 (1997).
- <sup>13</sup>J. J. Blanco, L. Lezama, M. Insausti, J. Gutierrez, J. M. Barandiaran, and T. Rojo, *Chem. Mater.* **11**, 3464 (1999).
- <sup>14</sup>K. Ghosh, S. B. Ogale, R. Ramesh, R. L. Greene, T. Venkatesan, K. M. Gapchup, R. Bathe, and S. I. Patil, *Phys. Rev. B* **59**, 533 (1999).
- <sup>15</sup>S. Hebert, A. Maignan, C. Martin, and B. Raveau, *Solid State Commun.* **121**, 229 (2002).
- <sup>16</sup>M. A. Gilleo, *Acta Crystallogr.* **10**, 161 (1957).
- <sup>17</sup>K. Ueda, H. Tabata, and T. Kawai, *Phys. Rev. B* **60**, R12561 (1999).
- <sup>18</sup>K. Ueda, Y. Muraoka, H. Tabata, and T. Kawai, *Appl. Phys. Lett.* **78**, 512 (2001).
- <sup>19</sup>R. D. Shannon, *Acta Crystallogr., Sect. A: Found. Crystallogr.* **A32**, 751 (1976).
- <sup>20</sup>K. De, R. Ray, R. N. Panda, S. Giri, H. Nakamura, and T. Kohara, *J. Magn. Magn. Mater.* **288**, 339 (2005).
- <sup>21</sup>P. A. Joy, Y. B. Khollam, and S. K. Date, *Phys. Rev. B* **62**, 8608 (2000).
- <sup>22</sup>V. L. Joseph Joly, P. A. Joy, S. K. Date, and C. S. Gopinath, *Phys. Rev. B* **65**, 184416 (2002).
- <sup>23</sup>P. A. Joy, Y. B. Khollam, S. N. Patole, and S. K. Date, *Mater. Lett.* **46**, 261 (2000).
- <sup>24</sup>W. Tong, B. Zhang, S. Tan, and Y. Zhang, *Phys. Rev. B* **70**, 014422 (2004).
- <sup>25</sup>Y. Wu, Z. Yu, and S. Liu, *J. Solid State Chem.* **112**, 157 (1994).
- <sup>26</sup>P. A. Joy and S. K. Date, *J. Magn. Magn. Mater.* **218**, 229 (2000).
- <sup>27</sup>F. M. A. Da Costa and A. J. C. Dos Santos, *Inorg. Chim. Acta* **140**, 105 (1987).
- <sup>28</sup>L. Fournes, Y. Potin, J. C. Grenier, G. Demazeau, and M. Pouchard, *Solid State Commun.* **62**, 239 (1987).
- <sup>29</sup>Z. Klencsar, Z. Nemeth, A. Vertes, I. Kotsis, M. Nagy, A. Cziraki, C. Ulhaq-Bouillet, V. Pierron-Bohnes, K. Vad, S. Meszaros, and J. Hakl, *J. Magn. Magn. Mater.* **281**, 115 (2004).
- <sup>30</sup>Zs. Gercsi, F. Mazaleyrat, S. N. Kane, and L. K. Varga, *Mater. Sci. Eng., A* **375-377**, 1048 (2004).
- <sup>31</sup>G. V. S. Rao, C. N. R. Rao, and J. R. Ferraro, *Appl. Spectrosc.* **24**, 436 (1970).
- <sup>32</sup>V. L. Joly, S. D. Bhame, P. A. Joy, and S. K. Date, *J. Magn. Magn. Mater.* **261**, 433 (2003).
- <sup>33</sup>H. Tanaka, N. Okawa, and T. Kawai, *Solid State Commun.* **110**, 191 (1999).